

# Superconducting Super Collider Laboratory

SSCL-Preprint-147



## Papers Contributed to the 1992 Applied Superconductivity Conference

The Magnet Test Analysis Group

August 1992

**Papers Contributed to the 1992 Applied  
Superconductivity Conference**

The Magnet Test Analysis Group

Accelerator Design and Operations Division  
Superconducting Super Collider Laboratory<sup>†</sup>  
2550 Beckleymeade Ave.  
Dallas, TX 75237

August 1991

---

<sup>†</sup>Operated by the Universities Research Association, Inc., for the U.S. Department of Energy under Contract No. DE-AC35-89ER40486.

# Current Dependence of Harmonic Field Coefficients of 5-cm-Aperture, 15-m-Long SSC Dipole Magnet Prototypes\*

Y. Zhao,<sup>1</sup> A. Akhmetov,<sup>1</sup> M. Anerella,<sup>2</sup> R. Bossert,<sup>3</sup> T. Bush,<sup>1</sup> D.W. Capone II,<sup>1</sup> J. Carson,<sup>3</sup> R. Coombes,<sup>1</sup> J. Cottingham,<sup>2</sup> S.W. Delchamps,<sup>3</sup> A. Devred,<sup>1</sup> J. DiMarco,<sup>1</sup> G. Ganetis,<sup>2</sup> M. Garber,<sup>2</sup> C. Goodzeit,<sup>1</sup> A. Ghosh,<sup>2</sup> S. Gourlay,<sup>3</sup> A. Greene,<sup>2</sup> R. Gupta,<sup>2</sup> R. Hanft,<sup>3</sup> A. Jain,<sup>2</sup> S. Kahn,<sup>2</sup> E. Kelly,<sup>2</sup> W. Koska,<sup>3</sup> M. Kuchnir,<sup>3</sup> J. Kuzminski,<sup>1</sup> M.J. Lamm,<sup>3</sup> P. Mantsch,<sup>3</sup> P.O. Mazur,<sup>3</sup> G. Morgan,<sup>2</sup> J. Muratore,<sup>2</sup> W. Nah,<sup>1,5</sup> T. Ogitsu,<sup>1,4</sup> D. Orris,<sup>3</sup> J. Ozelis,<sup>3</sup> T. Peterson,<sup>3</sup> E.G. Pewitt,<sup>3</sup> A. Prodehl,<sup>2</sup> M. Puglisi,<sup>1</sup> P. Radusewicz,<sup>1</sup> M. Rehak,<sup>2</sup> E.P. Rohrer,<sup>2</sup> J. Royet,<sup>6</sup> W. Sampson,<sup>2</sup> P. Sanger,<sup>1</sup> R. Scanlan,<sup>6</sup> R. Schermer,<sup>1</sup> R. Shutt,<sup>2</sup> R. Stiening,<sup>1</sup> J. Strait,<sup>3</sup> C. Taylor,<sup>6</sup> R. Thomas,<sup>2</sup> P. Thompson,<sup>2</sup> J.C. Tompkins,<sup>1</sup> J. Turner,<sup>1</sup> M. Wake,<sup>1,4</sup> P. Wanderer,<sup>2</sup> E. Willen,<sup>2</sup> Y. Yu,<sup>1</sup> J. Zbasnik,<sup>1</sup> and H. Zheng<sup>1</sup>

<sup>1</sup> Superconducting Super Collider Laboratory, Dallas, TX 75237 USA

<sup>2</sup> Brookhaven National Laboratory, Upton, NY 11973 USA

<sup>3</sup> Fermi National Accelerator Laboratory, Batavia, IL 60510 USA

<sup>4</sup> KEK, National Laboratory for High Energy Physics, Tsukuba, Ibaraki 305 Japan

<sup>5</sup> Korea Electrotechnology Research Institute, Changwon, Kyongnam 641-120, Korea

<sup>6</sup> Lawrence Berkeley Laboratory, Berkeley, CA 94720 USA



## ABSTRACT

Eighteen 5-cm-aperture, 15-m-long SSC dipole magnet prototypes have been produced and cold tested. On each prototype, the dependence of harmonic field coefficients on magnet current was measured as part of a study of the magnetic field quality. For most of the magnets, the observed behavior conforms to what can be expected from the effects of persistent magnetization currents and iron yoke saturation. A few prototypes, however, exhibited anomalies during current ramp at 4 A/s which can be attributed to large cable eddy currents.

## INTRODUCTION

The field produced by superconducting magnets has mainly three components: 1) a component,  $B_t$ , resulting from the transport current,  $I$ , circulating in the coil, 2) a component,  $B_m$ , resulting from persistent magnetization currents circulating in the superconducting filaments, and 3) a component,  $B_e$ , resulting from cable eddy currents. The  $B_t$  component only depends on the coil geometry and is expected to vary linearly as a function of  $I$ . The  $B_m$  component is dominated by the critical current density of the superconductor, which depends on the temperature and the magnetic field, and is expected to decrease as a function of  $I$ . The  $B_e$  component, however, only arises when the current is changed, and is expected to vary linearly as a function of  $(dI/dt)$ . In addition, magnetization of the iron yoke and of the cryostat vessel enhances each of the field components. The iron and cryostat contributions are expected to follow the same dependence as the coil contributions, except at high transport currents, where saturation effect result in sizable distortions.

In this paper, we review the current dependence of the harmonic field coefficients measured on 5-cm-aperture, 15-m-long SSC dipole magnet prototypes. Over the last year and half, eighteen full-length prototypes have been produced and cold-tested at Brookhaven National Laboratory (BNL) and Fermi National Accelerator Laboratory (FNAL). The BNL and FNAL magnets rely on the same magnetic design,<sup>1</sup> but differ in some of their mechanical features.<sup>2</sup> For the BNL magnets,

the yoke is split horizontally, and the collared-coil assembly is designed to interfere positively with the yoke along the vertical diameter. For the FNAL magnets, the yoke is split vertically, and the collar-yoke interference is along the horizontal diameter. After recalling a few definitions and describing the measurement procedure, we successively discuss the effects of persistent magnetization currents, eddy currents, and iron and cryostat magnetization. When appropriate, we also compare the behavior of the SSC dipole magnets to that of the superconducting dipole magnets for HERA.

## DEFINITIONS AND MEASUREMENT PROCEDURE

In the long, almost straight, section of the magnet, the field can be considered as two-dimensional, and is conveniently represented by a multipole expansion

$$B_y + iB_x = 10^{-4} B_0 \sum_{n=0}^{+\infty} (b_n + ia_n) \left( \frac{x+iy}{r_0} \right)^n, \quad (1)$$

where  $B_x$  and  $B_y$  are the  $x$ - and  $y$ -components of the field,  $B_0$  is the dipole field strength,  $b_n$  and  $a_n$  are the normal and skew  $2(n+1)$ -pole coefficients, and  $r_0$  is the reference radius. (For the SSC magnets,  $r_0 = 1$  cm.) The symmetry of a dipole magnet is such that only even normal multipole coefficients, also called *allowed* multipole coefficients, are non-zero. In real magnets, manufacturing errors result in violations of the dipole symmetry which lead to non-zero *un-allowed* multipole coefficients.

An extensive set of magnetic measurements is performed on each of the SSC dipole magnet prototypes that are produced. For the full-length prototypes, the field harmonics are measured using the *mole* system developed by BNL.<sup>3</sup> This system consists of a tangential coil and two dipole bucking coils, which are 0.6 m in length, and rotate with a 3.2 s period. The measured data are corrected for centering errors of the mole using the feed-down from the 18- or 22-pole.

The measurements are taken following a test sequence which is representative of a SSC main ring operating cycle. The sequence starts with a *cleansing quench* to erase all previous magnetization currents. The magnet is then pre-cycled to a current of 6500 A, for a duration of 5 min, simulating a

\*This work is supported by the U.S. Department of Energy under Contract No. DE-AC35-89ER40486.

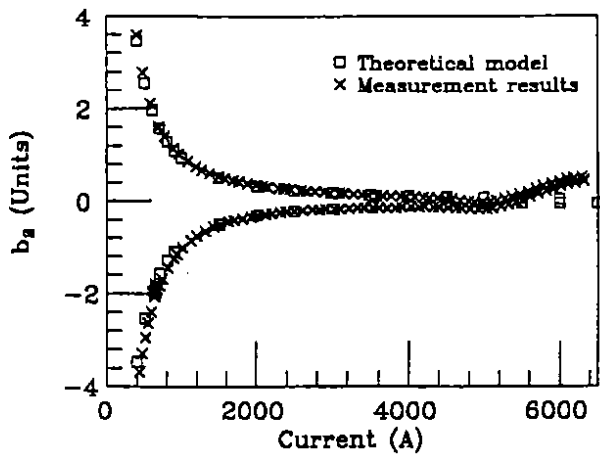


Fig. 1. Comparison between calculation and measurements of  $b_2$  vs. current for FNAL magnet DCA317 at 4.35 K.

colliding beam cycle. It is then ramped down to 115 A for a 2-min dwell, ramped up to 620 A and for a 10-min *pre-injection porch*, and ramped up again to 635 A for a 1-hour *injection porch*. At the end of the injection porch, the current is ramped up again to 6500 A, and then ramped down to 115 A, to simulate the next colliding beam cycle. The current ramp rate is 4 A/s, except for the ramp from 620 to 635 A, which is performed at 1 A/s. The data presented here paper include all the measurements taken starting from the 115-A dwell following the pre-cycle until the end of the test sequence.

#### EFFECTS OF PERSISTENT MAGNETIZATION CURRENTS

Persistent magnetization currents are generated at the periphery of the superconducting filaments in order to shield the filaments cores from the changes in local field resulting from current ramping. The magnetization currents form at the critical current density of the superconductor, and distribute themselves in order to produce, within the filaments, a dipole field opposite to the change in local  $B_T$ . Each filament, with its shells of persistent magnetization currents, then behaves as a magnetic doublet which slightly distorts the central field. Note, however, that the orientation of these magnetic doublets is determined by the transport-current flux lines, and thus, only the allowed multipole coefficients are expected to be affected.

Numerous models have been developed in order to predict the effects of persistent magnetization currents on the magnetic field. One of the most successful is that developed at Deutsches Elektronen-Synchrotron Laboratory (DESY), which reliably predicted the behavior of the superconducting magnets for HERA.<sup>4</sup> The same model is applied here toward understanding the persistent magnetization current effects in the SSC dipole magnets.

Figure 1 displays a comparison between calculation (squares) and measurements (crosses) of the normal sextupole coefficient ( $b_2$ ) versus current for FNAL magnet DCA317 at 4.35 K. The calculation relies on the DESY model and uses actual values of critical current densities measured on short samples of the cables wound in magnet DCA317. To allow a direct comparison, the geometric component was subtracted,

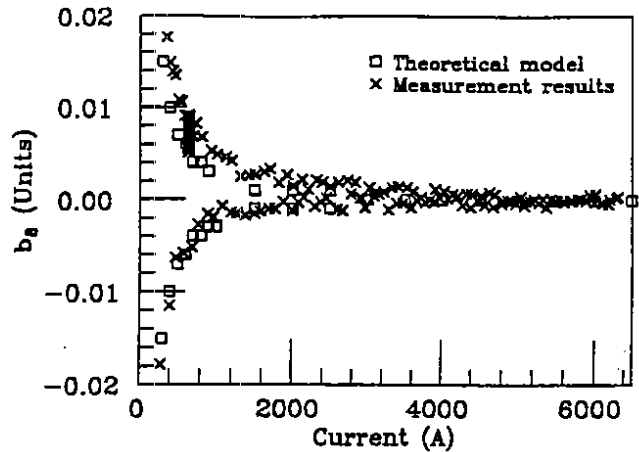


Fig. 2. Comparison between calculation and measurements of  $b_8$  vs. current for FNAL magnet DCA317 at 4.35 K.

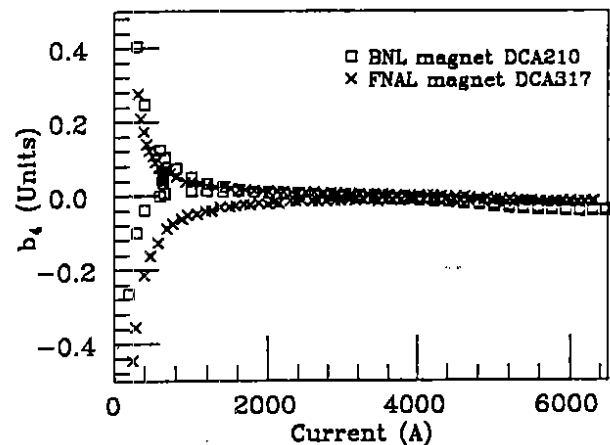


Fig. 3. Comparison of  $b_4$  vs. current measurements for BNL magnet DCA210 and FNAL magnet DCA317 at 4.35 K.

*i.e.*, the traces were shifted along the y-axis so that the average value between the two branches of the hysteresis is roughly zero. (For the two traces of Fig. 1, the lower branch corresponds to the current up-ramp; for currents above 4 kA, the experimental data show a clear rise, which, as discussed below, is attributed to iron yoke saturation effects.) Calculation and measurements are in good agreement. With the exception of the normal decapole coefficient ( $b_4$ ) for the BNL magnets, a similar agreement is observed for all even normal multipoles where the model predicts persistent magnetization currents effects. The agreement remains good even for high order multipoles where the amplitude of the effect is quite small. Figure 2 shows, for instance, a comparison between calculation and measurements of the normal 18-pole coefficient ( $b_8$ ) versus current for the same magnet and the same run as in Fig. 1. (For the two traces of Fig. 2, the upper branch correspond to the current up-ramp.) The data in Fig. 2 suggest that the random error of the measuring system can be estimated to be of the order of 0.002 units.

As we already mentioned, the only significant discrepancy that we observed between prediction and measurements is for the normal decapole coefficient ( $b_4$ ) of the BNL magnets. As an illustration, Fig. 3 shows a comparison between

measurements on BNL magnet DCA210 (squares) and measurements on FNAL magnet DCA317 (crosses). (For the two traces of Fig. 3, the upper branch corresponds to the current up-ramp.) The  $b_4$  hysteresis of the FNAL magnets appears symmetrical and in reasonable agreement with the prediction. The  $b_4$  hysteresis of the BNL magnet, however, exhibits a sizable asymmetry between the up-and down-branches. Such asymmetry is observed on all the BNL magnets, and its origin is not yet understood.

### EFFECTS OF CABLE EDDY CURRENTS

In the previous section, we discussed the effects of persistent magnetization currents, and we showed that, in most cases, there was a good agreement between theoretical predictions and measurement results. However, four dipole magnet prototypes (DCA312, DCA313, DCA314, and DCA315) exhibited field variations during current ramp at 4 A/s which significantly differed from the other prototypes, and which cannot be explained by the persistent magnetization current model.<sup>5</sup> It was also observed that this anomalous behavior only appeared while ramping the current, and that it ceased when the ramp was stopped.

In addition to this anomalous field behavior, these four magnets exhibited a dramatic degradation of their quench current as a function of ramp rate,<sup>6</sup> as well as large AC-losses.<sup>7</sup> A common feature of these four magnets is that they use inner cables made with strands coming from the same production batch of the same strand manufacturer. The strong ramp rate sensitivity and the large AC losses are attributed to unexpectedly large cable eddy currents,<sup>6</sup> and it is likely that these eddy currents are also responsible for the anomalous field behavior.<sup>5</sup>

The inner (outer) cables used in SSC magnets consist of 30 (36) bare strands, twisted together, and shaped into a flat, two-layer, slightly keystone cable. The cable mid-thickness is smaller than twice the strand diameter, and the contact surfaces at the crossovers between the strands of the two layers are relatively large. Also, during magnet assembly the coils are pre-compressed azimuthally.<sup>2</sup> Large pressures are thus applied perpendicularly to the cables, which keep the strands firmly in contact. The large contact surfaces and high pressures eventually result in low contact resistances at the strand crossovers, which couple the cable strands. Loops are thus formed where significant eddy currents can take place when subjected to a varying field. Assuming that the eddy currents flowing from one strand to the other always pass through the crossover resistance, the cable can be represented as a simple network of resistances. The cable eddy currents, and their effects on the magnetic field, can then be computed by combining this model circuit with a two-dimensional field calculation.<sup>5</sup>

Eddy-current fields arise when the transport current,  $I$ , is changed, and they are expected to vary linearly as a function ( $dI/dt$ ). In the first approximation, a current ramp at a constant rate should result in a constant eddy current field. Furthermore, if we assume that the crossover resistance,  $r_c$ , is uniform throughout the coil, the eddy current distribution follows the dipole symmetry and only effects the allowed multipole

coefficients. For a 5-cm-aperture SSC dipole magnet, the eddy-current sextupole and decapole fields at a 1-cm radius,  $B_{2e} = B_0 b_{2e}$  and  $B_{4e} = B_0 b_{4e}$ , can be estimated to be<sup>8</sup>

$$B_{2e}(r_0 = 1 \text{ cm}) = 0.4 (dI/dt)/r_c \quad , \quad (2a)$$

$$B_{4e}(r_0 = 1 \text{ cm}) = -0.02 (dI/dt)/r_c \quad , \quad (2b)$$

where  $B_{2e}$  and  $B_{4e}$  are in Gauss,  $dI/dt$  is in A/s, and  $r_c$  is in  $\mu\Omega$ . The corresponding power per unit length,  $W$ , dissipated by the eddy currents in the crossover resistances is

$$W = 2.5 \times 10^{-3} (dI/dt)^2 / r_c \quad , \quad (2c)$$

where  $W$  is in W/m

As a comparison, estimates of the same quantities for a HERA dipole magnet are (in the same units as above)<sup>8</sup>

$$B_{2e}(r_0 = 2.5 \text{ cm}) = 0.4 (dI/dt)/r_c \quad , \quad (3a)$$

$$B_{4e}(r_0 = 2.5 \text{ cm}) = -0.05 (dI/dt)/r_c \quad , \quad (3b)$$

$$W = 1.0 \times 10^{-3} (dI/dt)^2 / r_c \quad . \quad (3c)$$

The cables used in the HERA magnets have their strands coated with a thin layer of 95 wt% silver-5 wt% tin solder called *stabrite*. The purpose of this coating is to prevent the uncontrolled formation of a copper oxide layer at the strand periphery, and to make the crossover resistance as uniform as possible along the cable and throughout the cured coil. The drawback, however, is that it yields a low value of  $r_c$ . Measurements on a short sample of HERA cable show  $r_c = 2.1 \pm 0.5 \mu\Omega$ .<sup>9</sup> Introducing this number in Eq. (3a) lets us predict  $\Delta B_{2e}(r_0 = 2.5 \text{ cm}) = 0.2 \text{ Gauss/(A/s)}$ . Measurements that were recently performed on a HERA dipole magnet showed indeed  $\Delta B_{2e}(r_0 = 2.5 \text{ cm}) = 0.2 \text{ Gauss/(A/s)}$ .<sup>10</sup> This good agreement between calculation and measurements gives us some confidence that the model that was developed<sup>5</sup> can adequately predict the effects of cable eddy currents.

Unlike the HERA cables, the strands of the SSC cables are bare. They are thus free to develop a layer of copper oxide during the various steps of cable manufacturing and magnet assembly. Little is known, however, on the parameters that determine the thickness of this layer. Speculations are that it strongly depends on the purity of the copper matrix and whether the strands are annealed after the final drawing. It is also believed that the copper oxide layer depends strongly on the parameters of the coil curing cycle. In principle, the presence of this copper oxide layer can yield crossover resistances that are several orders of magnitude larger than that obtained with *stabrite*-coated strands. The drawback, however, is that it is difficult to control, and can lead to non-uniformities, either along the cable length, or from turn to turn in the cured coil. A distribution of crossover resistance that varies from turn to turn, as a function of the azimuth, results in an eddy-current distribution that violates the dipole symmetry, thereby effecting all multipole coefficients.

Figure 4 shows a summary plot of skew quadrupole coefficient ( $a_1$ ) versus current for two anomalous SSC dipole magnet prototypes (magnets DCA314 and DCA315) compared to a normally-behaved one (magnet DCA317). Although we are not expecting any sizable effects from the persistent magnetization currents, magnets DCA314 and DCA315 both

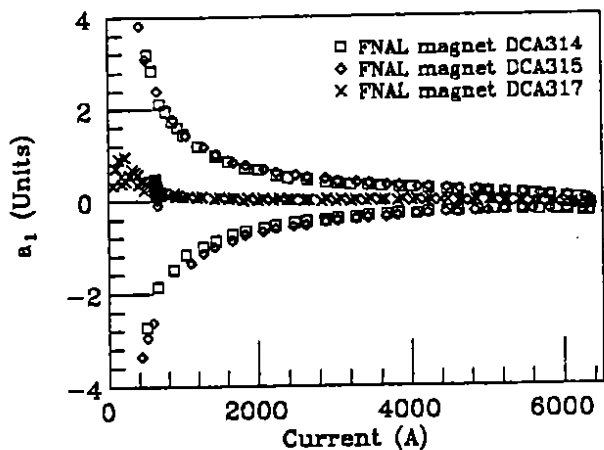


Fig. 4: Summary of  $a_1$  vs. current for two anomalous magnets (magnets DCA315 and DCA314) and a normally-behaved one (magnet DCA317).

exhibit a very large hysteresis. Furthermore, these two hystereses appear to be described in opposite direction: for magnet DCA314, the current up-ramp corresponds to the upper branch, while, for magnet DCA315, it corresponds to the lower branch. As described in reference 5, this anomalous  $a_1$  behavior can be explained in terms of top/bottom asymmetric eddy currents resulting from a non-uniform distribution of crossover resistances. (For currents above 4 to 5 kA, the three traces of Fig. 4 show a tendency to dip, which, as described below, is attributed to flux leakage asymmetry between magnet cold mass and cryostat.)

For each of the anomalous magnets, it is in fact possible to determine an azimuthal distribution of crossover resistance, that results in a distribution of eddy currents, which can explain the observed behavior of all the multipole coefficients and is consistent with the measured AC-losses.<sup>5</sup> Also, for each of the anomalous magnets, the model accurately predicts in which half coil the high ramp rate quenches should originate. This consistent agreement between simulations and experimental data gives us good confidence that we have identified the cause of the poor AC performance of these four magnets. Efforts are now underway to determine how to avoid these non-uniformities in the crossover resistance.

#### EFFECTS OF IRON YOKE AND CRYOSTAT

Above 4 kA, the transport-current field produced by the coil is large enough to saturate the iron yoke. Due to a high field at the pole, iron saturation is first felt there, which results in a positive contribution to the normal sextupole coefficient ( $b_2$ ). The return flux through the midplane causes it to saturate as well. At currents of the order of 6500 A, midplane saturation overcomes pole saturation resulting in a net negative  $b_2$ . The present magnetic design, however, includes cut-outs at the midplane of the iron yoke that are designed to force the midplane saturation to occur at a lower current, and thus to compensate partially the effect on  $b_2$  of the pole plane saturation.<sup>1</sup> This compensation was very successfully implemented on the BNL-design magnets, for which the  $b_2$  change due to iron saturation does not exceed 0.1 units. As can

be seen in Fig. 1, the FNAL-design magnets do exhibit a larger change (of the order of 0.5 units at 6500 A), but the observed  $b_2$  saturation conforms to prediction. The iron saturation also effects the normal decapole coefficient ( $b_4$ ), but to a lesser extent. For both designs, the observed  $b_4$  saturation conforms to prediction.

Another predicted effect is that, at high current, flux lines start to leak out of the cold mass. As the cold mass is not centered within the cryostat, and the cryostat itself is made of low carbon steel, the flux lines become slightly distorted. This distortion, which violates the top/bottom symmetry, results in a decrease of  $a_1$ <sup>11</sup> which, for the 5-cm-aperture dipole magnets, is estimated between 0.1 and 0.2 units. For the normally-behaved magnet of Fig. 4 (DCA317), the observed  $a_1$  saturation is within prediction.

#### CONCLUSION

For most of the 5-cm-aperture, 15-m-long SSC dipole magnet prototypes tested so far, the observed current dependence of the harmonic field coefficients can be described by persistent magnetization currents and of iron yoke and cryostat vessel magnetization. A few prototypes, however, exhibit anomalous behavior of their field harmonics during current ramp at 4 A/s. These anomalies, which cease when the current ramp is stopped, can be explained in terms of cable eddy currents. Efforts are now under way to determine the cable parameters that need to be mastered in order to control them.

#### REFERENCES

- 1 R.C. Gupta, S.A. Kahn, and G.H. Morgan, "SSC 50 mm Dipole Cross Section," *Supercollider 3*, J. Nonte, ed., 1991, pp. 587-599.
- 2 A. Devred, T. Bush, *et al.*, "Review of SSC Dipole Magnet Mechanics and Quench Performance," to appear in *Supercollider 4*, J. Nonte, ed., 1992.
- 3 G. Ganetis, J. Herrera, *et al.*, "Field Measuring Probe for SSC Magnets," Proc. 1987 IEEE Part. Acc. Conf., 1987, pp. 1393-1395.
- 4 H. Brück, D. Gall, *et al.*, "Persistent Magnetization Effects in the Superconducting HERA Magnets and Correction Coils," Proc. 2nd Eur. Part. Acc. Conf., 1990, pp. 1160-1162.
- 5 T. Ogitsu, Y. Zhao, *et al.*, presented at the ICFA workshop on AC Superconductivity, KEK, National Laboratory for High Energy Physics, Tsukuba, Japan, June 23-25, 1992.
- 6 W. Nah, A. Akhmetov, *et al.*, "Quench Characteristics of 5-cm-Aperture, 15-m-Long SSC Dipole Magnet Prototypes," in these Proceedings.
- 7 J. Ozelis, S.W. Delchamps, *et al.*, "AC Loss Measurements of Model and Full Size 50 mm SSC Collider Dipole Magnets at Fermilab," in these Proceedings.
- 8 T. Ogitsu, private communication.
- 9 A. Ghosh, private communication.
- 10 H. Brück, private communication.
- 11 R.C. Gupta, J.G. Cottingham, *et al.*, "A Comparison of Calculations and Measurements of the Field Harmonics as a Function of Current in the SSC Dipole Magnets," Proc. 1991 IEEE Part. Acc. Conf., 1991, pp. 42-44.